Electronic structure of Bi_2CuO_4

A. Goldoni and U. del Pennino

Dipartimento di Fisica, Università degli Studi di Modena, Via Campi 213/A, 41100 Modena, Italy

F. Parmigiani

Centro Informazioni, Studi ed Esperienze, Tecnologie Innovative S.p.A. Materials Division,
P.O. Box 12081, Milano, Italy
and Facoltà di Scienze, Università di Como, Como, Italy

L. Sangaletti

Dipartimento di Fisica "A. Volta" dell'Università, Via A. Bassi, 6, Pavia, Italy

A. Revcolevschi

Laboratoire de Chimie des Solides, Unité Associé au CNRS 446, Université de Paris-Sud, Bâtiment 414,
F-91405 Orsay Cédex, France

The electronic structure of a Bi_2CuO_4 single crystal is investigated by x-ray photoelectron (XPS), x-ray Auger-electron (XAES), and electron-energy-loss (EELS) spectroscopies. The analysis of the XPS and XAES data confirms that Bi_2CuO_4 is a charge-transfer insulator with a band gap of about 2 eV, while the Cu-O bond in Bi_2CuO_4 is more ionic than in CuO and the $Bi_2Sr_2CaCu_2O_{8-\delta}$ superconductor. Furthermore, the density of the empty states is tentatively described from a combined analysis of the EELS and XPS data and some electronic transitions are identified from the EELS spectra.

I. INTRODUCTION

The electronic structure of compounds with copper ions coordinated with four oxygens in a square-planar configuration has been the subject of considerable attention recently, since this structure is common to the majority of copper oxide based high-temperature superconductors (HTSC's). Bi_2CuO_4 belongs to this class of square-planar compounds but only little information is available about its electronic structure. Bi_2CuO_4 is a quasi-one-dimensional system with a $K_2Pt(CN)_4$ structure. Isolated CuO_4 square-planar units are stacked one above the other in a staggered fashion along the c axis. This structure forms one-dimensional chains of copper ions. The copper atoms are not bridged by any intervening oxygen or bismuth ions, and the Cu-Cu distance is only slightly larger than that observed in metallic copper.

Neutron and x-ray diffraction data, at 13 and 300 K,[1-3] polarized Raman and unpolarized infrared-reflectivity spectra,[4] suggest that the appropriate space group for the Bi_2CuO_4 crystal structure is $P4/ncc\,(D_{4h})$.

The presence of alkaline-earth ions in the Bi-Cu-O lattice dramatically influences the nature of the Cu-O bond, transforming Bi-Cu-O systems from charge-transfer insulators into high-temperature superconductors. In these systems superconductivity takes place in the Cu-O planes. Thus a comparative study of the nature of the Cu-O bonds in CuO, Bi_2CuO_4, $Bi_2Sr_2CaCu_2O_{8-\delta}$ (Bi2212), and other related compounds is important. The aim of this paper is to report and interpret spectroscopic data obtained by combined x-ray photoelectron spectroscopy (XPS), x-ray Auger-electron spectroscopy (XAES), and electron-energy-loss spectroscopy (EELS) for a high-quality Bi_2CuO_4 single crystal.

The experimental data, analyzed on the basis of an extension of the theory proposed in Refs. 5 and 6 for a CuO_4 cluster model, clearly indicate that Bi_2CuO_4 is a charge-transfer insulator with a gap of about 2 eV while the Cu-O bond is more ionic than in CuO and $Bi_2Sr_2CaCu_2O_{8-\delta}$. In addition, some electronic transitions are identified from the EELS spectra and the density of the empty states is tentatively described from a combined analysis of the EELS and XPS data.

II. EXPERIMENT

A high-quality Bi_2CuO_4 single crystal was grown from the melt by a floating zone technique associated with an image furnace using sintered rods prepared by solid-state reactions between CuO and Bi_2O_3 in a molar ratio 1:1.[7] A centimeter-sized Bi_2CuO_4 single crystal was then oriented on the basis of its Laue pattern and arranged on a sample holder to be cleaved perpendicular to the c crystal axis in ultrahigh vacuum conditions inside the analytical chamber. The cleavage plane was $\langle 100 \rangle$. XPS and EELS measurements were each performed in separate systems using different samples from the same Bi_2CuO_4 crystal. After the cleavages and during the whole set of experiments the residual pressure in the two chambers never exceeded $\approx 10^{-10}$ mbar.

XPS spectra were collected by exciting the sample with

a monochromatic Al $K\alpha$ x-ray source ($h\nu = 1486.6$ eV). The spectrometer was calibrated using the Ag Fermi edge, the Ag $3d_{5/2}$ core line, and the Cu $2p_{3/2}$ core line to which binding energies (BE's) of 0, 368.3, and 932.7 eV were assigned, respectively. The BE scale was then referred to the Bi $4f$ core line whose maximum was fixed at 158.8 ± 0.1 eV. By setting the spectrometer pass energy at ≈ 5 eV an overall resolution of ≈ 0.4 eV was obtained for the Ag $3d_{5/2}$ core line. An electron flood gun was used to reduce surface electrostatic charging during the XPS measurements.

EELS were obtained in a different apparatus equipped with a low-energy electron diffraction (LEED) system and an Auger spectrometer to control the surface quality. A normal-incidence electron gun was used for the electron energy loss experiment, while the reflected electrons were collected using a double-pass cylindrical mirror analyzer. The EELS were detected using an energy of the primary e^- beam of $E_0 = 200$ and 2000 eV. The total resolution of the EEL spectra was estimated to be ≈ 0.7 eV.

Using a primary beam energy of 165 eV the LEED images obtained for a cleaved Bi_2CuO_4 surface exhibited a diffraction pattern consistent with that expected from the Bi_2CuO_4 (001) surface.[8] LEED images could not be obtained for a beam energy below 150 eV because of sample charging effects. At higher beam energies the LEED spots were very broad.

III. RESULTS AND DISCUSSION

A. XPS core lines

The O$1s$ XP spectrum shows a symmetric line for which a maximum is found at 530 ± 0.1 eV. The full width at half maximum (FWHM) is ≈ 1 eV. These features, along with the lack of satellites on the high-BE side, as well as those observed in the O $1s$ XP spectra of CuO single crystal,[9] suggest a good quality of the crystal surface. It is interesting to note that the BE of the O $1s$ core line in Bi_2CuO_4 is ≈ 0.5 eV higher than in CuO. That could indicate a more covalent character of the Cu-O bond in Bi_2CuO_4 than in CuO, which is in contradiction with the results reported in this paper, as will be shown in the following. Figure 1(a) reports the XPS Cu $2p$ lines of Bi_2CuO_4. This spectrum exhibits satellite structures typical of divalent copper ions and a relatively narrow and symmetric main line.

An impurity cluster configuration-interaction model that includes the exchange and the spin-orbit interactions is used to analyze the Cu $2p$ XPS spectra.[5,6] The crystal structure of Bi_2CuO_4 is particularly suitable for the use of this method since Cu^{2+} ions are located at the center of four square-planar-coordinated oxygen atoms and the resulting D_{4h} symmetry represents very well the local symmetry of copper in Bi_2CuO_4.

In this light the multiplet splitting for an ionic, unscreened, pd (e.g., $2p^5 3d^9$) configuration are calculated using the following parameters: $F^2(2p,3d) = 7.47$ eV, $G^1(2p,3d) = 5.62$ eV, $G^3(2p,3d) = 3.21$ eV, $\zeta_d = 0.13$ eV and $\zeta_p = 13.6$ eV obtained by atomic numerical Hartree-
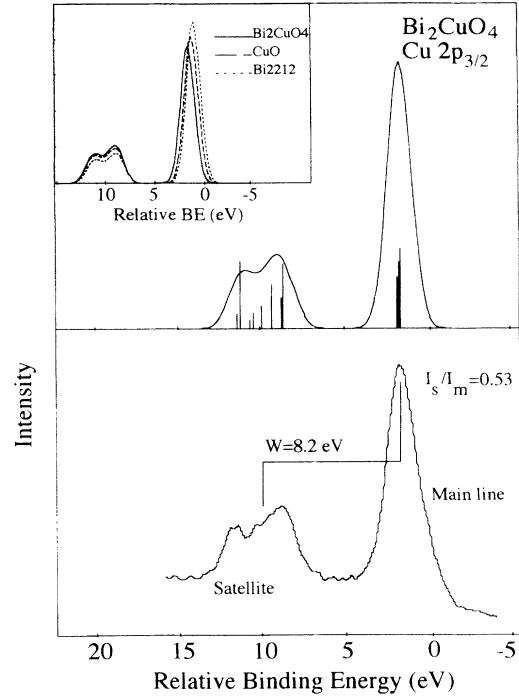
FIG. 1. Lower panel: Cu $2p_{3/2}$ XP spectrum. Upper panel: Cu $2p_{3/2}$ calculated XP spectrum for Bi_2CuO_4. The eight multiplet splitting components, both in the satellite and in the main line, are evidenced with vertical bars. Inset: Cu $2p_{3/2}$ calculated XP spectrum for Bi_2CuO_4, CuO, and Bi2212.

Fock calculations. The eigenvalues, obtained through a 12×12 matrix diagonalization,[10] give the spin-orbit and exchange contributions, $Q_{S.O./ex}$, to Q_{pd}. Q being the Coulomb part of the two-hole pd Slater integral, Q_{pd} can be calculated from the following equation:

$$Q_{pd}^{(i)} = Q + Q_{S.O./ex}^{(i)} \quad (i = 1, \ldots, 12) . \tag{1}$$

Among the 12 eigenvalues, four are derived from the $j_p = \frac{1}{2}$ spin-orbit coupling and eight from the $j_p = \frac{3}{2}$ spin-orbit coupling. For the analysis of the Cu $2p_{3/2}$ spectrum the charge transfer is accounted for by a 2×2 matrix associated with each of the eight Q_{pd} relevant values. To simplify the analysis the charge transfer energy Δ and the mixing matrix element of the Hamiltonian, T, are assumed to be independent of the crystal field as well as the O $2p$ band dispersion.

The separation between the centroid of the main and satellite lines, W, and the satellite to main line intensity ratio, I_S/I_M, is given by

$$I_S/I_M = \Sigma I_S^{(i)} / \Sigma I_M^{(i)} \tag{2}$$

and

$$W = E_S - E_M = \frac{1}{I_S} \sum_i E_S^{(i)} I_S^{(i)} - \frac{1}{I_M} \sum_i E_M^{(i)} I_M^{(i)} , \tag{3}$$

where i ranges from 1 to 8.

The set of Δ, T, and Q parameters that gives a calculated W and I_S/I_M closest to the measured values was chosen as representative for $Bi_2 CuO_4$.[11]

Table I reports the Δ, T, and Q calculated values for the set of cuprates considered in this paper. Δ is the parameter showing the most remarkable variation. Differences in Δ reflect the different environment in which the Cu-O cluster is embedded.[12] As Torrance and Metzeger observed,[13] Δ is primarily influenced by changes in Madelung energies associated with out-of-plane structural variations. On the other hand, the higher the Δ the more difficult it is to populate the $3d^{10}\underline{L}$ configuration, where $\underline{L}$ denotes a hole in the lingand orbital. Therefore, variations of Δ influence the I_S/I_M ratio. For this reason, the main line intensity decreases with respect to the satellite intensity when Δ becomes larger.

In Bi₂CuO₄, the charge transfer Δ has the highest value. Figure 1(b) shows the Cu $2p_{3/2}$ XPS core line calculated for Bi₂CuO₄ using the parameter reported in Table I. It is clear in this compound the main line to satellite intensity is the smallest, as well as the energy separation W [see the Bi2212 data reported in the inset of Fig. 1(b)] and, on the basis of this analysis, Bi₂CuO₄ is a more ionic compound than CuO and Bi2212. If one assumes that BE shifts are correlated with atomic charges, this result is in contrast with the trend observed for the BE maximum of the O $1s$ core lines measured on Bi₂CuO₄, CuO, and Bi2212 which suggests as more ionic the Cu-O bond in Bi2212. However, since several initial- and final-state effects influence the measured kinetic energy of the O $1s$ photoelectrons the analysis reported in this paper is more complete and detailed.

The variation of T is correlated, in first approximation, to the Cu-O nearest-neighbor distance $(d_{\text{Cu-O}})$ used to simulate the cluster. Since T varies as $(d_{\text{Cu-O}})^{-4}$ (Ref. 14) the calculated T values are consistent with $d_{\text{Cu-O}}$, as shown in Table I. Instead, as expected, the Q values are nearly the same for the five compounds under examination, since Q is a Coulomb interaction localized on the photoemitting copper site.

From the observation of the satellite line shape, some important questions should be raised. In fact, the satellite shape is remarkably different within the cuprate family. It is known that multiplet splitting accounts for the broad and complex satellite shape.[5] However, in the present case, the three calculated satellite shapes look

quite similar in contrast with the experimental results [inset of Fig. 1(b)]. In particular, the difference of the satellite structure observed in Bi₂CuO₄ with respect to CuO and Bi2212 suggests a different hybridization strength and anisotropy between the former compounds and Bi₂CuO₄.[6,15] Also the main line shows different FWHM and different degrees of asymmetry. The asymmetry of the main line can be ascribed, in a first degree approximation, to multiplet splitting effects. Though this effect is more enhanced for the satellite, where the unscreened $|2p^5 3d^9\rangle$ configuration has the dominant weight, the multiplet splitting can propagate, through hybridization, to the main line. However, the multiplet splitting alone does not account for the considerable width observed in the Cu $2p$ XPS Bi2212 and La₂CuO₄ main lines.[12] The strong asymmetry, and consequently the increased width, is fully accounted for only when the O $2p$ band dispersion is considered, as Kotani[5] have shown for the Cu $2p$ XPS spectra of CuO and La₂CuO₄.

B. The U_{dd} correlation energy

Another important parameter necessary to understand the electronic properties of cuprates is the correlation energy U_{dd}. It is possible to acquire information about the d-d correlation energy form the Cu core-VV Auger lines, since these transitions leave the system with three $3d$ holes. Figure 2 shows the Cu $L_3M_{4,5}M_{4,5}$ Auger lines of Bi₂CuO₄, which originate from the decay of the hole in the Cu $2p_{3/2}$ orbital, where a main peak (marked M) and a shoulder (marked S) are well visible.

The main peak corresponds to the Auger transition starting from the ionic state $|\Psi_M\rangle$ and ending in a three-holes final state with a dominant $|2p^6 3d^8\underline{L}\rangle$ configuration,

$$|\Psi_M\rangle \cong |2p^5 3d^{10}\underline{L}\rangle \Longrightarrow |2p^6 3d^8\underline{L}\rangle , \qquad (4)$$

while the shoulder corresponds to the Auger transition starting from the ionic state $|\Psi_S\rangle$ and ending in a three-hole final state with a dominant $|2p^6 3d^7\rangle$ configuration,

$$|\Psi_S\rangle \cong |2p^5 3d^9\rangle \Longrightarrow |2p^6 3d^7\rangle . \qquad (5)$$

Considering the kinetic energies of the electrons emitted

TABLE I. Results of the CI-cluster model study. The satellite to main line intensity I_S/I_M ratio, the calculated T, D, and Q_{pd} parameters, as well as the number of $3d$ electrons in the ground state, and the nearest-neighbor Cu-O distance are reported.

		I_S/I_M	W (eV)	T (eV)	Δ (eV)	Q (eV)	n_d (GS)	$d_{\text{Cu-O}}$ (Å)
Bi2212	expt.	0.35	8.7					1.91
	calc.	0.36	8.7	2.25	1.65	7.8	9.33	
Bi₂CuO₄	expt.	0.53	8.2					1.94
	calc.	0.54	8.2	2.00	2.15	8.0	9.26	
CuO	expt.	0.46	8.7					1.95
	calc.	0.47	8.54	2.00	1.75	8.0	9.30	
La₂CuO₄	expt.	0.38	8.6					1.90
	calc.	0.38	8.7	2.25	1.75	7.9	9.32	
Nd₂CuO₄	expt.	0.35	9.45					1.97
	calc.	0.37	9.2	1.90	1.00	8.1	9.37	
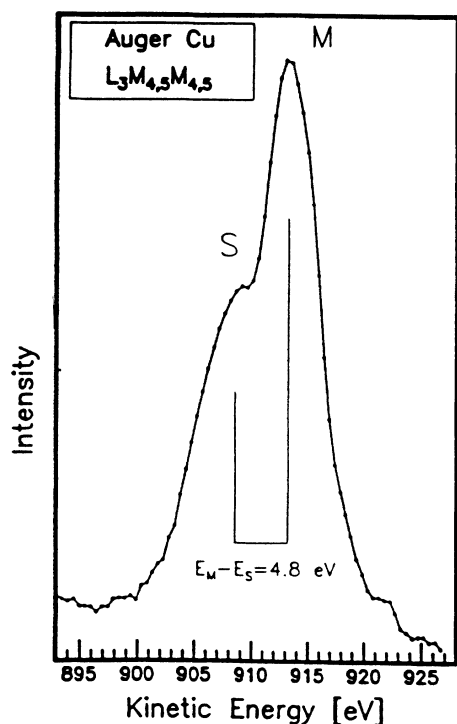
FIG. 2. Cu $I_3 M_{4,5} M_{4,5}$ Auger lines observed in the x-ray excited spectra of Bi_2CuO_4. The energy separation between satellite and main peak positions (vertical lines) is also reported.

from the (3.4) and (3.5) transitions, it is possible to estimate the separation between the main peak and the shoulder as follows:[5]

$$E_M - E_S \sim 2U_{dd} - Q \ . \tag{6}$$

Using a Q experimental value of ≈ 8 eV, and a $E_M - E_S$ of ≈ 4.8 eV (see Fig. 2), a U_{dd} energy of ≈ 6.4 eV is obtained.

C. Valence band and empty states: Photoemission and EEL spectra

The Bi_2CuO_4 valence band is reported in Fig. 3(a). Two main structures are clearly observed. The more intense extends from 1 to 8 eV, while a second, less intense emission, ranges from 8 to 14 eV. The low-BE emission presents three features at 3.5 (A'), 4.5 (B'), and 6.5 eV (C'). Also the high-BE valence-band region appears structured. Two features at 11 (D') and at 13 eV (E') are clearly detected.

The Bi_2CuO_4 XPS density of states (XPS-DOS) resembles those obtained from HTSC's and CuO. Nevertheless, some differences are observed. To discuss these differences, the CuO single-crystal valence-band spectrum is reported [Fig. 3(b)]. The CuO valence-band spectrum can also be divided into two regions ranging approximately from 1 to 8 eV and from 8 to 18 eV, with the addition of a significant component between 5–9, labeled C.

The CuO valence-band main line exhibits two predominant features. A main component (B) at 3.5 eV and a should (A) at 1.5 eV. The satellite structure, in the
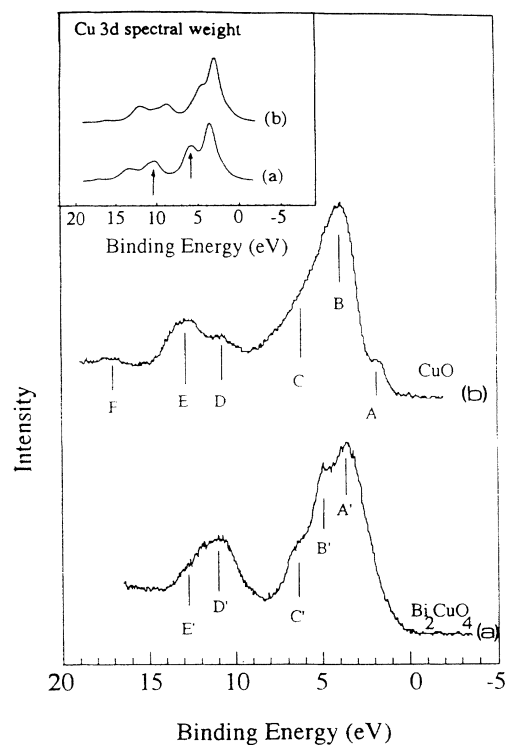
FIG. 3. Bi_2CuO_4 and CuO valence-band XP spectra. Inset: calculated Cu $3d$ spectral weight for a $[CuO_4]^{6-}$ cluster (see Ref. 19). Case (a) corresponds to a 2.4-eV energy gap, while (b) corresponds to a 1.8-eV energy gap.

8–18-eV BE range, also shows two features at 10.5 (D) and 12.5 eV (E). Finally, a high-BE contribution F is found at 17.5 eV.

Valence-band (VB) resonant photoemission measurements[16] and the comparison between VB-XPS and VB-UPS spectra[17] explain the Cu character of the high-BE satellite (8–18 eV). On the basis of these experiments, the low-BE structure is attributed to the contribution of strongly hybridized Cu-O states, while A and F are the $^1A_{1g}$ symmetry Cu-O hybridized states.[17,18]

The same assignment can be extended to Bi_2CuO_4, although differences in the fine-structure details with respect to CuO exist. The comparison between CuO and Bi_2CuO_4 provides interesting information. In CuO the main line is asymmetric, but not structured, whereas, in Bi_2CuO_4 the main line has two extra features B' and C'. On the contrary, the satellite structures are similar, but the intensity ratio of the two features, i.e., D,E and D',E', appearing in the XPS spectra is reversed. Moreover, in Bi_2CuO_4 the counterpart of the CuO A and F features is not detected, within the limits of the present measurements.

These findings have a correspondence in the results reported in a theoretical study[19] where impurity-cluster configuration interaction calculations are performed to fit the CuO VB data. Using a symmetry-dependent Cu $3d$–O $2p$ hybridization and treating the d-d Coulomb and exchange interactions within the full atomic multiplet theory, the CuO VB spectrum is studied in detail. To fit the data, different sets of parameters are used.

From each set, a value for the energy gap is also obtained. The best agreement between the experimental data and the calculated $3d$ spectral weight is achieved by a parameter set corresponding to a 1.8-eV energy gap. Increasing the energy gap (2.4 eV), an increase of the central region of the calculated Cu $3d$ spectral weight is observed. The inset of Fig. 3 reports the results relative to the 1.8-eV and 2.4-eV gap. In particular, as indicated by the arrows, the 2.4-eV gap spectrum shows a double featured main line with a considerable increase of the high-BE peak and an intensity increase on the low-BE side of the satellite.

These results agree with the trend experimentally observed in the XPS-DOS spectra going from CuO to Bi_2CuO_4. In particular, they account for the increased emission detected in the VB central region, 5–11 eV, of Bi_2CuO_4. This agreement allows us to estimate an energy gap of ≈ 2.4 eV for Bi_2CuO_4.

A larger band energy gap in Bi_2CuO_4 than in CuO can be deduced also from the core level estimated Δ values (see Table I). In fact, the energy gap in these cuprates roughly scales as Δ (apart from hybridization shifts and bandwidths) and the calculated Δ for Bi_2CuO_4 is larger than the Δ value obtained for CuO.

A last remark concerns the Bi contribution to the VB states. The Bi $6s$ cross section is very low at x-ray energies, but the Bi $6s$ level mixes strongly with O $2p$ levels and a weak contribution to the valence spectral weight is expected. For these reasons, further fine-structure discrepancies between the experimental data and the total Cu-O spectral weight around the structures at 7.5 (peak D) and 2 eV could be attributed to Bi-O states (Bi $6s$–O $2p$ bonding and antibonding states and Bi $6s$ nonbonding states) which obviously are not present in the $[CuO_4]^{6-}$ cluster.

To gain further information about the Bi_2CuO_4 valence-band electronic structure, electron-energy-loss spectra were measured and studied. EELS spectra result from the convolution of the densities of the filled with the empty states. Therefore the origin of some spectral structures is sometimes ambiguous. On the other hand, the comparison with the photoemission spectra and the dependence of the EELS spectra of the energy of the primary beam can contribute to eliminate many ambiguities. In this case EELS measurements are a powerful technique to acquire information on both the filled and empty states.

The discussion will be limited to the description of the main features in the EELS spectrum of Bi_2CuO_4 (Fig. 4) at $Ep = 2$ keV and its second derivative $(-d^2N/dE^2)$, in the energy region 0–40 eV, while a more detailed analysis has been published separately.[20]

Nine peaks, labeled as A'–I', are detected. Most of them arise from interband transitions, plasmon excitations, and shallow core electron excitations and their assignment takes into account the present photoemission spectra, the inverse photoemission (IPS), and bremsstrahlung isochromatic (BIS) spectra of Bi2212 (Refs. 21 and 22) and the EELS spectra of Bi_2O_3,[23] Bi2212,[24–26] and $Bi_2(Sr,Ca)_3CuO_2O_Y$ (Ref. 23) reported in literature.

The EELS spectrum of Bi_2CuO_4 is very similar to that

of Bi_2O_3 (inset of Fig. 4), indicating that the excitations from the Bi-O orbitals are dominant. Accordingly, the peaks at higher loss energies, i.e., G' (26.8), H' ($\sim$29.4), and I' ($\sim$31.6 eV), correspond to the transitions from the Bi $5d$ levels to the unoccupied Bi $6p$ states. On the basis of the constant final-state spectroscopy (Ref. 27) and the vacuum ultraviolet reflectivity spectra[28] of Bi_2O_3, peaks H' and I' are assigned to the Bi $5d_{3/2} \rightarrow$ Bi $6p_{1/2}$ and Bi $5d_{3/2} \rightarrow$ Bi $6p_{3/2}$ transitions, respectively. Instead, peak G' is attributed to the Bi $5d_{5/2} \rightarrow$ Bi $6p_{1/2,3/2}$ transitions, where the dipole-forbidden coupling with the $6p_{1/2}$ state is not negligible. The XPS measurements reported in the present work show the Bi $5d_{3/2,5/2}$ doublet at $\sim$28.5 and $\sim$25.5 eV BE. As a consequence, the unoccupied Bi $6p$ levels should be located between 1.5–3 eV above the Fermi energy E_F. This result does not agree with BIS and IPS data[21,22] for Bi2212, where the centroid of the Bi $6P$ empty levels is found $\sim$4 eV above E_F. Similar disagreements are present also in other EELS (Ref. 24) and optical reflectivity spectra[21,28] of Bi-oxide based compounds. A possible explanation arises if an excitoniclike mechanism that produces a downward shift of 1.5–2 eV is considered for the EELS spectra of Bi_2CuO_4. If this interpretation is correct, this final-state effect reflects the strong Coulomb interaction between $5d$ and $6p$ states.

According to Fujimori et al.[23] the double peaks B' ($\sim$6.1–4.4 eV) and C' ($\sim$9.9–8.2 eV) are assigned to
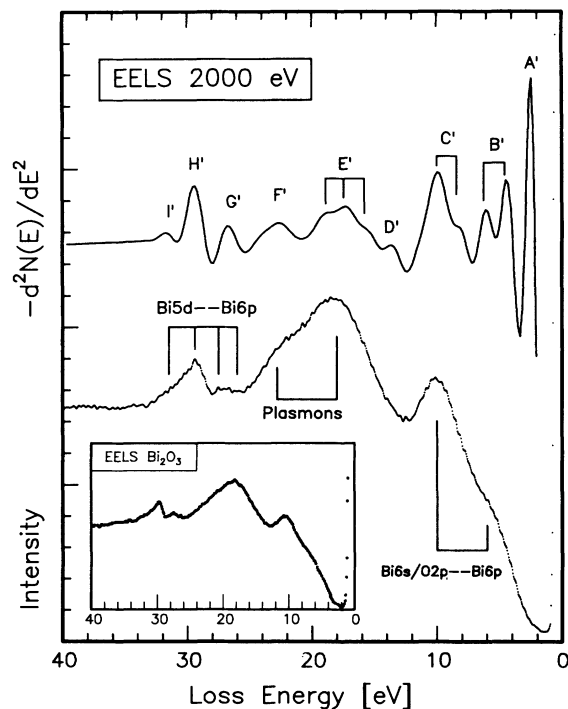
FIG. 4. EEL spectrum of Bi_2CuO_4, and its second derivative, in the energy-loss region 0–40 eV, obtained with primary energy $E_P = 2000$ eV. Some electronic transitions and the plasmons are also indicated. The inset shows the EEL spectrum of Bi_2O_3 (Ref. 23) obtained with the same primary energy.

the transitions from the hybridized Bi $6s$–O $2p$ antibonding and bonding states (VB region) to the empty Bi $6p$ states. If the Bi $6p$ bands are within 3 and 5 eV above E_F, then the bonding and antibonding Bi-O states are, respectively, $\sim$5 and $\sim$1.5 eV below E_F. These peaks have a one-to-one correspondence with the fine structure observed in the XPS VB spectrum.

If the interpretation that the bonding states have strong O $2p$ character is correct,[20,21,23] a strong contribution of oxygen to the XPS VB spectrum is expected in the region around 5 eV [structures B' and C' of Fig. 3(a)]. Besides, the position of the antibonding states suggests a Bi $6s$ contribution at the top of the valence band at about 1.5 eV below E_F.

Peak A' ($\sim$2.4 eV) is clearly seen in the second derivative and it could correspond to the one-electron excitation from the top of the valence band to the bottom of the conduction band; therefore its energy position should be a measure of the Bi_2CuO_4 energy gap ($Eg \leq 2.4$ eV). Remembering that the present XPS analysis gives $\Delta = 2.15$ eV, this corresponds well to the charge transfer nature of the gap in Bi_2CuO_4 and it is also in good agreement with the estimate based on the VB-spectra analysis. A 2.7-eV feature has been observed[29,30] in the EELS spectra of the Bi-based HTSC compounds, which corresponds to the 2.4-eV feature of the Bi_2CuO_4 spectrum. Some investigators[30] suggested that this excitation might be the excitonic counterpart of a 3.6-eV charge-transfer feature (also observed in the EELS spectra of the Bi-based HTSC compounds), but this last feature was not observed in Bi_2CuO_4.

The prominent structure in the center of the spectrum (12–25 eV loss energy) is dominated by the plasmon excitations, but there are also some electronic transitions which can fall around these loss energies.

The volume plasmon excitation of valence electrons corresponds to structure F' ($\sim$22.6 eV). In fact a crude determination of plasmon energy (using $N = 148$ electrons per unit cell, $e_\infty = 1$ and the cell parameter given in Ref. 1) gives $\hbar\omega_p \approx 22$ eV which is very close to the energy position of peak F'. This interpretation is also supported by the fact that on going from $Ep = 2$ keV to $Ep = 200$ eV (Ref. 20) its intensity is strongly reduced. Since the O $2s$ level is observed at $\sim$21-eV BE by XPS, also the transition O $2s \rightarrow$ (Cu $3d$–O $2p$)* at the bottom of the conduction band (1–2.5 eV above E_F for Bi2212 compounds[20,21]) can contribute to the energy-loss spectrum around 23 eV.

Between 16 and 20 eV (peak E') the surface plasmon and the electron excitations from the filled O $2p$ levels to the unoccupied O-$3sp$ hybridized states in the higher conduction band [11–14 eV above E_F (Ref. 16)] should occur. Shoulder D' (13.6 eV) can be tentatively assigned to the transition from the nonbonding Bi $6s$ orbitals (8–10 below E_F) to the Bi $6p$ levels. Also the transitions from the large Cu $3d$ band to the empty Cu $4p$ levels, located around 10 eV above E_F,[16] could contribute to peak D'.

Finally, on the basis of the filled-state energy positions deduced from direct photoemission and of the values of
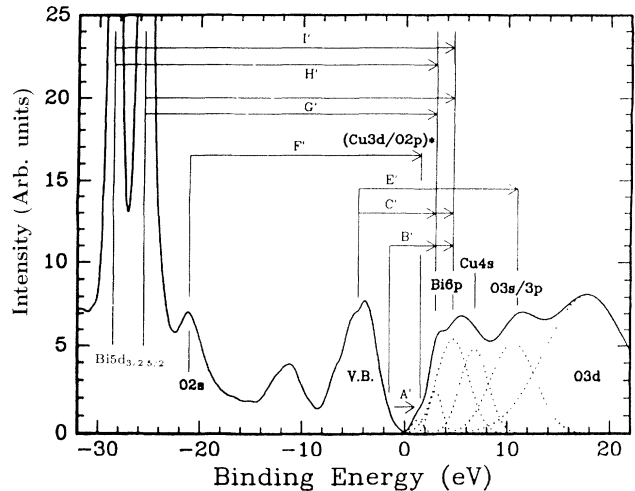
FIG. 5. Density of filled and empty states as deduced from XPS and EELS data of Bi_2CuO_4. The Gaussians (dotted lines) tentatively indicate the positions and width of each empty state, while their convolution is reported as a solid line, above BE equal to 0. Below 0 are plotted the filled states obtained by XPS.

the energy transitions obtained from EELS, a tentative density of empty states was deduced. These states are shown in Fig. 5 as dotted Gaussian together with their convolution (solid line). Also reported are the photoemission lines and the principal EELS transitions.

IV. CONCLUSIONS

Analyzing the XPS and XAES spectra of Bi_2CuO_4, this material is found to be a charge-transfer insulator with a gap greater than 2 eV and a set of electronic parameters consistent with those obtained for Bi2212 and CuO. With respect to the nature of the Cu-O bond, Bi_2CuO_4 results to be more ionic than CuO and Bi2212. The necessity of accounting for the O $2p$ band dispersion in a realistic calculation of Cu $2p$ line shape is stressed. In Bi_2CuO_4 this dispersion is lower than in Bi2212 and La_2CuO_4.

Further information about the electronic structure of Bi_2CuO_4 has been obtained from EELS spectra. In particular it has been shown that the transition involving the Bi-derived states dominates the EELS spectrum. Furthermore, a contribution of the Bi $6s$ orbital to the top of valence band and in the VB region around 7 eV, suggested from the comparison between CuO and Bi_2CuO_4 XPS VB spectra, has been confirmed by EELS measurements. The EELS spectrum also indicate an energy-gap value of about 2.4 eV (apart from excitonic effect). Finally a tentative density of empty states has been deduced from XPS and EELS results.

ACKNOWLEDGMENTS

[1]J. L. Garcia-Muñoz, J. Rodriguez-Carvajal, F. Sapina, M. J. Sanchis, R. Ibañez, and D. Beltran-Portez, J. Phys. Condens. Matter **2**, 2205 (1990).

[2]J. P. Attfield, J. Phys. Condens. Matter **1**, 7045 (1989).

[3]E. W. Ong, G. H. Kwei, R. A. Robinson, B. L. Ramakrishna, and R. B. Von Dreele, Phys. Rev. B **37**, 4255 (1990).

[4]Z. V. Popovic, G. Kliche, M. Cardona, and R. Liu, Phys. Rev. B **41**, 3824 (1990).

[5]G. van der Laan, C. Westra, C. Haas, and G. A. Sawatzyk, Phys. Rev. B **23**, 4369 (1981); see also *Core Level Spectroscopy in Condensed Systems*, edited by J. Kanamori and A. Kotani, Solid-State Science Vol. 81 (Springer-Verlag, Berlin, 1987); A. Kotani and K. Okada, Prog. Theor. Phys. Suppl. **101**, 329 (1990).

[6]F. Parmigiani and L. Sangaletti, Chem. Phys. Lett. **213**, 613 (1993).

[7]G. Dhalenne, A. Revcolevschi, M. Aln, B. Hennion, G. Andre, and G. Parette, Cryst. Prop. Prep. **35-36**, 11 (1991).

[8]K. Shredhar, P. Ganguly, and S. Ramasesha, J. Phys. C **21**, 1129 (1988).

[9]F. Parmigiani, G. Pacchioni, F. Illas, and P. S. Bagus, J. Electron. Spectrosc. Rel. Phenom. **59**, 255 (1992).

[10]E. U. Condon and G. H. Shortley, *The Theory of Atomic Spectra* (Cambridge University Press, Cambridge, 1964).

[11]A. K. Santra, D. D. Sarma, and C. N. R. Rao, Phys. Rev. B **43**, 5621 (1991). For Nd$_2$CuO$_4$ see also H. Ishii, T. Koshizawa, H. Kataura, T. Hanyu, H. Takai, K. Mizogouchi, K. Kume, I. Shiozaki, and S. Yamaguchi, Jpn. J. Appl. Phys. **28**, L1952 (1989).

[12]F. Parmigiani, L. E. Depero, T. Minerva, and J. Torrance, J. Electron. Spectrosc. Relat. Phenom. **58**, 315 (1992).

[13]J. R. Torrance and R. M. Metzeger, Phys. Rev. Lett. **63**, 1515 (1989).

[14]W. A. Harrison, *Electronic Structure and the Properties of Solids* (Dover, New York, 1964).

[15]K. Okada and A. Kotani, J. Electron. Spectrosc. Relat. Phenom. **52**, 313 (1990).

[16]J. Ghijsen, L. H. Tjeng, H. Eskes, G. A. Sawatzky, and R. L. Johnson, Phys. Rev. B **42**, 2268 (1990).

[17]H. Eskes, L. H. Tjeng, and G. A. Sawatzky, Phys. Rev. B **41**, 288 (1990).

[18]J. Ghijsen, L. H. Tjeng, J. van Elp, H. Eskes, J. Westerink, G. A. Sawatzky, and M. T. Czyzyk, Phys. Rev. B **38**, 11 322 (1988).

[19]Z.-X. Shen, R. S. List, D. Dessau, F. Parmigiani, A. J. Arko, R. Bartlett, B. O. Wells, I. Lindau, and W. E. Spicer, Phys. Rev. B **42**, 8081 (1990).

[20]A. Goldoni, U. del Pennino, F. Parmigiani, and A. Revcolevschi, Solid State Commun. **90**, 161 (1994).

[21]A. E. Bouquet, S. Ogawa, H. Eisaki, H. Takagi, S. Uchida, A. Fujimori, and S. Suga, Physica C **169**, 1 (1990).

[22]T. J. Wagener, Yongjun Hu, Y. Gao, M. B. Jost, J. H. Weaver, N. D. Spencer, and K. C. Goretta, Phys. Rev. B **39**, 2928 (1989); see also T. J. Wagener, Yongjun Hu, M. B. Jost, J. H. Weaver, Y. F. Yan, X. Chu, and Z. X. Zhao, *ibid.* **42**, 6317 (1990).

[23]A. Fujimori, S. Takekawa, E. Takayama-Muromachi, Y. Uchida, A. Ono, T. Takahashi, Y. Okabe, and H. Katayama-Yoshida, Phys. Rev. B **39**, 2255 (1985).

[24]A. Ando, K. Saiki, A. Koma, H. Eisaki, and Shin-ichi Uchida, Jpn. J. Appl. Phys. **30**, L1371 (1991).

[25]V. A. Grazhulis and A. M. Ionov, J. Electron. Spectrosc. Relat. Phenom. **52**, 375 (1990).

[26]Z.-X. Shen, P. A. P. Lindberg, D. S. Dessau, I. Lindau, W. E. Spicer, D. Z. Mitzi, I. Bozovic, and A. Kapitulnik, Phys. Rev. B **39**, 4295 (1989).

[27]Z. Hurysch and R. L. Benbow, Phys. Rev. Lett. **38**, 1094 (1977).

[28]A. A. Agasiev, V. E. Bagiev, A. M. Mamedov, and Ya.Yu. Guseinov, Phys. Status. Solidi B **149**, K191 (1988).

[29]M. K. Kelly, P. Barboux, J.-M. Tarascon, and D. E. Aspenes, Phys. Rev. B **40**, 6797 (1989).

[30]Y.-Yu Wang and A. L. Ritter, Phys. Rev. B **43**, 1241 (1991).